Journal of Computational and Applied Mathematics 413 (2022) 114399

Contents lists available at ScienceDirect

Journal of Computational and Applied Mathematics

journal homepage: www.elsevier.com/locate/cam

The stability of a dynamic duopoly Cournot–Bertrand game model

Yu Yu *

School of Economics, Zhejiang University of Finance & Economics, Hangzhou, Zhejiang, 310018, China
Center for Economic Behavior and Decision-making, Zhejiang University of Finance & Economics, Hangzhou, Zhejiang, 310018, China

ARTICLE INFO

Article history:
Received 23 March 2021
Received in revised form 3 March 2022

JEL classification:
D21
D43
C73

Keywords:
Global stability
Cournot–Bertrand model
Dynamic game
Neimark–Sacker bifurcation
Chaos

ABSTRACT

The paper is devoted to exploring the complex dynamics of a Cournot–Bertrand model, where one agent chooses quantity and the other chooses price. A nonlinear discrete system is built to illustrate the game model with bounded rationality. Theoretically, the local and global stability of equilibrium are investigated. The simulation reveals that Flip and Neimark–Sacker bifurcation phenomena occur when the adjustment speed of one firm increases through different boundary curves. Therefore three different chaotic attractors are presented. The standard Logistic mapping is applied to analyze the dynamics of the system on invariant axes. The critical curves classify the number of preimage of the quantity or price. Besides, simulations give more intuitive results: the cycle attractor, chaotic attractor and the basin of attraction with "holes" are given.

1. Introduction

The oligopoly is a market organization between perfect competition and monopoly. Cournot model was the first duopoly model proposed in 1838 [1]. In this model, both companies sell homogeneous goods and compete for quantity. While sometimes firms take a price decision. In a Bertrand model, when both players' price was equated with their marginal cost, the Bertrand equilibrium was produced [2]. It means that the firms' long-term profits are zero, which is a conclusion of the perfect market. The Stackelberg model described a two-stage game, where one leader moved first and all other followers moved after him [3].

In game theory, Nash equilibrium is a traditional core concept. While in recent years, game model combined with chaos theory is applied to analyze the stability region of the equilibrium. This topic attracts more scholars' concern. The dynamics of duopoly game was investigated with incomplete rational players [4–6]. Under the assumption of naïve rationality, adaptive expectation, bounded rationality, bounded rationality with delay and local monopolistic approximation, the stability region could be enlarged by the bounded rationality with delay [7,8]. In classical Cournot, Bertrand and Stackelberg models, the equilibrium eventually entered chaos via bifurcation which was caused by the adjustment speed of output or price [9–11].

Generally, quantity and price competition coexist in a dynamic economy system. Besides classical game models, the Cournot–Bertrand mixed model was proposed. Singh and Vives [12] analyzed the duality of price and quantity in differentiated duopoly. They showed that, under specific assumptions about the cost (i.e., zero fixed cost and constant

* Correspondence to: School of Economics, Zhejiang University of Finance & Economics, Hangzhou, Zhejiang, 310018, China
E-mail address: yyuu_123@126.com.

https://doi.org/10.1016/j.cam.2022.114399
0377-0427/

marginal cost) the Cournot–Bertrand "hybrid" competition cannot endogenously prevail. Tremblay and Tremblay [13] established a static Cournot–Bertrand model for oligopolistic markets with product differentiation. Their theoretical analysis suggested that sufficient product differentiation was a necessary condition to ensure the equilibrium of the two types of products, and only Cournot-type firm survived when there was no product differentiation. Naimzada and Tramontana [14] adopted adaptive adjustments and generalized the static Cournot–Bertrand model to the dynamic Cournot–Bertrand model. They pointed out that the adaptive adjustment mechanism can lead to the instability of Nash equilibrium. Semenov and Tondji [15] compared the equilibrium, consumer surplus and social welfare in Cournot and Bertrand model. Tremblay and Tremblay's [16] work is the review of Cournot–Bertrand model, the development and contribution of the model.

The above researches on Cournot–Bertrand games mainly focused on theoretical analysis. Some scholars have studied the local stability properties of equilibrium, and the results of numerical simulations have verified the theoretical results. Ma et al. [17] established a Cournot–Bertrand model with market share preference. The instability had opposite effects on firms with quantity and price decision. The stability region of Cournot–Bertrand model was bigger than that of Cournot or Bertrand system under the same conditions [18,19]. The equilibria of Cournot, Bertrand, and Cournot–Bertrand model were compared [20]. Our work extends the work of these literature, and along this direction, the gradient adjustment mechanism is used to analyze the local and global stability properties in Cournot–Bertrand type game models. The stability region of the equilibrium is presented. Flip and Neimark–Sacker bifurcation occur when the parameter exceeds the boundary of the stability region. The Logistic mapping is used to analyze the dynamics property of the Cournot–Bertrand model in invariant axes. We divide several regions, each with the same number of preimages. It is convenient for finding different basins of attraction.

In this paper, the gradient adjustment mechanism is adopted to establish a dynamic Cournot–Bertrand model, and a detailed theoretical analysis and numerical simulation are carried out on the stability of the attractor, and a more complex stable region of the Nash equilibrium is given. The model in this paper is based on a more general consumer utility function. To make the conclusion of the article more economically meaningful, we have introduced a feasible set of consumer strategies. Combined with the feasible set of strategies, the structure of the attractor's domain of attraction is analyzed from the perspectives of theory and numerical simulation.

A Cournot–Bertrand model with linear cost is considered. The assumption of vertical differentiation products is to avoid that the market share is occupied by the firm which has a lower price. The local and global stability of the dynamic game model are analyzed. In Section 2, the Nash equilibrium of the static duopoly Cournot–Bertrand model is investigated. In Section 3, the two firms have the same bounded rationality. The local stability of the dynamic Cournot–Bertrand model is analyzed. In Section 4, the theoretical results of Section 3 are verified by the simulation. In Section 5, the theoretical result of global stability of the dynamic Cournot–Bertrand model is concluded. In Section 6, we give the numerical simulation of Section 5. In Section 7, the conclusion is presented.

2. The Nash equilibrium of the static duopoly Cournot–Bertrand model

In a duopoly market, two firms provide two products with vertical differentiation, whose quantities are $q_i, i = 1, 2$. The representative consumer has the quadratic utility function, where the utility function is more general than that of Andaluz and Jarne [21]:

$$U(q_1, q_2) = \alpha_1 q_1 + \alpha_2 q_2 - 1/2(\beta_1 {q_1}^2 + 2rq_1q_2 + \beta_2 {q_2}^2),$$

where the parameters are satisfied:

$$\alpha_i, \beta_i > 0, \beta_1\beta_2 - r^2 > 0, \alpha_i\beta_j - r\alpha_j > 0, i, j = 1, 2, i \neq j \tag{1}$$

Consumers choose p_i $(i = 1,2)$ according to $p_i = \partial U/\partial q_i$. Therefore the inverse demand function is

$$\begin{cases} p_1 = \alpha_1 - \beta_1 q_1 - rq_2 \\ p_2 = \alpha_2 - \beta_2 q_2 - rq_1 \end{cases} \tag{2}$$

α_i characterizes the price cap of product i when $q_1 = 0, q_2 = 0$. The bigger α_i is, the higher the welcome level of product i. β_i means the effect of the variation of q_i on p_i. r describes the effect of the variation of q_j on p_i. r is the substitution parameter of the two products which measures the substitution ability. $r > 0, r = 0, r < 0$ represents the substitution, independence and complementation relationship between two products, respectively. Especially, when $\alpha_1 = \alpha_2$, $\beta_1 = \beta_2 = r$, in this situation, homogeneous products with completely substitutable are obtained. Assuming $\beta_1\beta_2 - r^2 > 0$, that is the products have differentiation.

Refer to Andaluz and Jarne [21], we have the transformation as follows:

$$\sigma = \beta_1\beta_2 - r^2, a_i = (\alpha_i\beta_j - \alpha_j r)/\sigma, b_i = \beta_j/\sigma, c = r/\sigma, i, j = 1, 2, i \neq j \tag{3}$$

The demand function is rewritten as

$$\begin{cases} q_1 = a_1 - b_1 p_1 + cp_2 \\ q_2 = a_2 - b_2 p_2 + cp_1 \end{cases} \tag{2'}$$

where a_i is the demand cap of product i, b_i denotes the effect of variation of $p_i$on q_i, c represents the effect of variation of p_i on q_j.

We have the transformation as follows:

$$\delta' = b_1b_2 - c^2, \alpha_i = (a_ib_j + a_jc)/\delta', \beta_j = b_j/\delta', r = c/\delta', i, j = 1, 2, i \neq j \tag{3'}$$

Then the inverse demand function (2) transforms into the demand function (2′).

It is assumed that the marginal cost of firm i is $m_i > 0$, replace $\alpha_i - m_i$ with α_i, replace $a_i - b_im_i + cm_j$ with a_i, thus the two firms have the profit function with the same form: $\pi_i = p_iq_i, i = 1, 2$.

In Cournot–Bertrand model, firm 1 chooses q_1, firm 2 chooses p_2, from the first formula of demand function (2′) and the second formula of demand function (2), we have

$$p_1 = (a_1 - q_1 + cp_2)/b_1$$

$$q_2 = (\alpha_2 - rq_1 - p_2)/\beta_2$$

Since $p_1 \geq 0, q_2 \geq 0$, the strategy combination (q_1, p_2) satisfies the feasible set:

$$\Omega = \{q_1 \geq 0, p_2 \geq 0 \,|\, a_1 - q_1 + cp_2 \geq 0, \alpha_2 - rq_1 - p_2 \geq 0\} \tag{4}$$

where (p_1, q_2) satisfies

$$\begin{cases} q_1 - cp_2 \leq a_1 \\ rq_1 + p_2 \leq \alpha_2 \\ q_1 \geq 0, p_2 \geq 0 \end{cases}$$

For the fixed p_2, firm 1 chooses q_1 to maximize $\pi_1(q_1, p_2)$, that is solving the optimization problems:

$$\max_{q_1} \pi_1 = p_1q_1 = (a_1 - q_1 + cp_2)q_1/b_1$$

The marginal profit function of firm 1 is

$$\partial\pi_1/\partial q_1 = (a_1 + cp_2 - 2q_1)/b_1 \tag{5}$$

For the fixed q_1, firm 2 chooses p_2 to maximize $\pi_2(q_1, p_2)$, that is solving the optimization problems:

$$\max_{p_2} \pi_2 = p_2q_2 = (\alpha_2 - rq_1 - p_2)p_2/\beta_2$$

The marginal profit function of firm 2 is

$$\partial\pi_2/\partial p_2 = (\alpha_2 - rq_1 - 2p_2)/\beta_2 \tag{5'}$$

Definition. q_1 and p_2, a_i and α_j, c and $-r$ are called duality variables. One expression with variables which are replaced by duality variables could become another expression. Both expressions are dual.

The two dual expressions are recorded as $(\cdot)$ and $(\cdot)'$.

Please note that α_i is $\alpha_i - m_i (i = 1, 2)$, p_2 is $p_2 - m_2$ actually.

The Nash equilibrium of the static Cournot–Bertrand is:

$$\begin{cases} {q_1}^* = (2a_1 + c\alpha_2)/(4 + cr) \\ {p_2}^* = (2\alpha_2 - ra_1)/(4 + cr) \end{cases} \tag{6}$$

where $({q_1}^*, {p_2}^*) \in \Omega$.

From formula (6), the effect of variation of some parameters on Cournot–Bertrand Nash equilibrium is concluded:

(1) When a_1 increases, ${q_1}^*$ increases, for $a_i = a_i - b_im_i + cm_j$, the product 1 is more popular with a lower the cost. The stronger the influence of price on the output of firm 1, the greater the equilibrium output of firm 1.

(2) The bigger α_2 is, if $c > 0$, that is the two products are alternatives, the bigger ${q_1}^*$ is; the bigger α_2 is, if $c < 0$, that is the two products are complements, the smaller ${q_1}^*$ is. Because α_2 is the price cap of p_2.

(3) The bigger α_2 is, the bigger ${p_2}^*$ is.

(4) The bigger a_1 is, if $r > 0$, that is the two products are alternatives, the smaller ${p_2}^*$ is; the bigger a_1 is, if $r > 0$, that is the two products are complements, the bigger ${p_2}^*$ is.

3. The local stability of equilibrium of the dynamic Cournot–Bertrand model with bounded rationality

In the static Cournot–Bertrand model, using Nash equilibrium to predict game results requires participants to have a high degree of rationality and information conditions about the market, which is difficult to achieve in the real economic environment. A more realistic condition is that participants only have limited rationality and limited information about the market. Under this more realistic condition, it is assumed that firms adjust their output and price dynamically through a gradient adjustment mechanism. Just like the importance of Nash equilibrium to static games, attractors play an important role in dynamic games. We examine the conditions of Nash equilibrium in Cournot–Bertrand model by gradual adjustment mechanism and the stability of other attractors.

In the dynamic Cournot–Bertrand model, firm 1 can only predict the gradient of profit with respect to quantity which is the marginal profit, no other information. When the marginal value which is expected is positive, firm 1 will increase the price of next period; otherwise it will reduce the price of next period. Therefore the following dynamic system can be used to describe the dynamic trajectory of the economic operation.

$$T_{c-b}:\begin{cases} {q_1}' = q_1 + v_1 q_1(a_1 + cp_2 - 2q_1)/b_1 \\ {p_2}' = p_2 + v_2 p_2(\alpha_2 - rq_1 - 2p_2)/\beta_2 \end{cases} \tag{7}$$

where $v_1 > 0$ is firm 1's adjustment speed of quantity, $v_2 > 0$ is firm 2's adjustment speed of price.

The fixed points of the mapping T_{c-b} can be solved by the algebraic equations:

$$\begin{cases} q_1(a_1 + cp_2 - 2q_1)/b_1 = 0 \\ p_1(\alpha_2 - rq_1 - 2p_2)/\beta_2 = 0 \end{cases}$$

They are $E_0 = (0, 0)$, $E_1 = (a_1/2, 0)$, $E_2 = (0, \alpha_2/2)$, $E_* = ({q_1}^*, {q_2}^*)$. Where E_0, E_1, E_2 are boundary equilibria, E_* is Nash equilibrium. ${q_1}^*, {q_2}^*$ are given by formula (6).

To discuss the asymptotic stability of the fixed points, the characteristic roots of Jacobian matrix $J(q_1, q_2)$ of the mapping T_{c-b} at $E_i(i = 0, 1, 2, ^*)$ are calculated.

$$J(q_1, p_2) = \begin{bmatrix} 1 + v_1(a_1 + cp_2 - 4q_1)/b_1 & v_1 q_1 c/b_1 \\ -v_2 p_2 r/\beta_2 & 1 + v_2(\alpha_2 - rq_1 - 4p_2)/\beta_2 \end{bmatrix} \tag{8}$$

From $J(E_0) = \begin{bmatrix} 1 + v_1 a_1/b_1 & 0 \\ 0 & 1 + v_2\alpha_2/\beta_2 \end{bmatrix}$, the two characteristic roots of $J(E_0)$ are $\lambda_1 = 1 + v_1 a_1/b_1 > 1$, $\lambda_2 = 1 + v_2\alpha_2/\beta_2 > 1$, therefore E_0 is repellent, that is the trajectory of the point starting near from E_0 moves away from E_0 as time increases.

From $J(E_1) = \begin{bmatrix} 1 - v_1 a_1/b_1 & v_1 a_1 c/2b_1 \\ 0 & 1 + v_2(\alpha_2 - ra_1/2)/\beta_2 \end{bmatrix}$, $J(E_1)$ has one characteristic root $\lambda_1 = 1 + v_2(\alpha_2 - ra_1/2)/\beta_2$, from the transformation (3′), $(\alpha_2 - ra_1/2)/\beta_2 = (2a_2 b_1 + a_1 c)/2\delta'\beta_2 > 0$, therefore $\lambda_1 > 1$. The other characteristic root $\lambda_2 = 1 - v_1 a_1/b_1 < 1$. When $v_1 < 2b_1/a_1$, $|\lambda_2| < 1$, E_1 is a saddle point. E_1 attracts along the horizontal direction and repels along the eigenvector direction of λ_1. When $v_1 > 2b_1/a_1$, E_1 is a repellent point. Similarly, when $v_2 < 2\beta_2/\alpha_2$, E_2 is also a saddle point. E_2 attracts along the vertical direction and repels along the eigenvector direction of ${\lambda_1}'({\lambda_1}' = 1 + v_1(a_1 + c\alpha_2/2)/b_1)$. When $v_2 > 2\beta_2/\alpha_2$, E_2 is a repellent point.

The locally asymptotic stability of Nash equilibrium E_* is analyzed in the following discussion. From the expression of E_* and formula (8), the Jacobian matrix of the mapping T_{c-b} at E_* is

$$J(E_*) = \begin{bmatrix} 1 - 2v_1{q_1}^*/b_1 & v_1 c{q_1}^*/b_1 \\ -v_2 r{p_2}^*/\beta_2 & 1 - 2v_2{p_2}^*/\beta_2 \end{bmatrix}$$

For convenience, let $x = v_1{q_1}^*/b_1$, $y = v_2{p_2}^*/\beta_2$, we have

$$J(E_*) = \begin{bmatrix} 1 - 2x & cx \\ -ry & 1 - 2y \end{bmatrix} \triangleq J_*$$

The trace of J_* is $T = 2 - 2x - 2y$. The determinant of J_* is $D = (1 - 2x)(1 - 2y) + crxy = T - 1 + wxy$, where $w = 4 + cr > 4$.

The Jury's condition of stability of E_* is

$$\begin{cases} (1)\, 1 - T + D > 0 \\ (2)\, 1 + T + D > 0 \\ (3)\, D < 1 \end{cases}$$

First, $1 - T + D = wxy > 0$, therefore the orbit of the mapping T_{c-b} will not produce transcritical bifurcation.

Second, the condition (2) $1 + T + D = 4 - 4x - 4y + wxy > 0$, which is equivalent to $y(4 - wx) < 4(1 - x)$.

Let $\bar{x} = w/4$, when $x < \bar{x}$, $y < (4(1 - x))/(4 - wx) \triangleq F(x)$. When $x > \bar{x}$, $y > F(x)$. Since $F'(x) = 4(w - 4)/(4 - wx)^2 > 0$, $F(x)$ is increasing monotonically. It is a hyperbola whose vertical and horizontal asymptote is $4/w$.

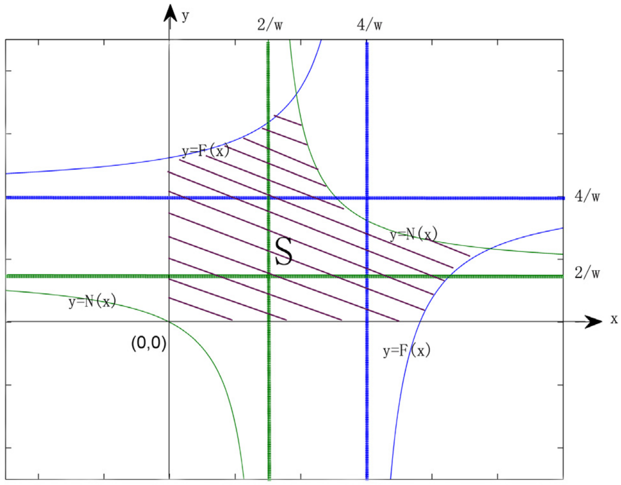

Fig. 1. The stability region S of E_*.

At last, the condition (3) is equivalent to $-2x-2y+xyw<0$, that is $y(xw-2)<2x$. Let $\tilde{x}=2/w$, therefore when $x<\tilde{x}$, $y>2x/(xw-2)\triangleq N(x)$. When $x>\tilde{x}$, $y<N(x)$. $N(x)$ is decreasing monotonically. It is a hyperbola whose vertical and horizontal asymptote is $2/w$.

From Jury's condition, the stability region S of E_* is surrounded by two axes, $F(x)$ and $N(x)$, which satisfies
when $0<x<x^-$, then $0<y<F(x)$,
when $x^-<x<1$, then $0<y<N(x)$,
when $1<x<x^+$, then $F(x)<y<N(x)$,
where $x^\pm=(w\pm\sqrt{w(w-4)})/w$ is the intersection of $F(x)$ and $N(x)$.
From $x=v_1q_1{}^*/b_1$, $y=v_2p_2{}^*/\beta_2$, $F(x)$ and $N(x)$, we have

$$F(v_1)=4\beta_2(1-v_1q_1{}^*/b_1)/(p_2{}^*(4-(4+cr)v_1q_1{}^*/b_1)),$$
$$N(v_1)=2\beta_2(v_1q_1{}^*/b_1)/(p_2{}^*((4+cr)v_1q_1{}^*/b_1-2)).$$

Easy to know, $F(v_1)$ is increasing monotonically, with vertical asymptote $v_1=\frac{4}{(4+rc)}\frac{b_1}{q_1{}^*}$, horizontal asymptote $v_2=\frac{4\beta_2}{p_2{}^*}\frac{1}{(4+rc)}$. $N(v_1)$ is increasing monotonically, with vertical asymptote $v_1=\frac{2}{(4+rc)}\frac{b_1}{q_1{}^*}$, horizontal asymptote $v_2=\frac{2\beta_2}{p_2{}^*}\frac{1}{(4+rc)}$.
In the v_1-v_2 coordinate system, the stability region satisfies
when $0<v_1<v_1^-$, then $0<v_2<F(v_1)$;
when $v_1^-<v_1<b_1/q_1{}^*$, then $0<v_2<N(v_1)$;
when $b_1/q_1{}^*<v_1<v^+$, then $F(v_1)<v_2<N(v_1)$.
Where $v^\pm=(1\pm\sqrt{\frac{cr}{4+cr}})b_1/q_1{}^*$ (see Fig. 1).
Based on the above analysis, two following positions are concluded:

Proposition 1. *In the dynamic Cournot–Bertrand model, the boundary equilibrium E_0 is repellent. When $0<v_1<2b_1/a_1$, $E_1=(a_1/2,0)$ is a saddle point; when $v_1>2b_1/a_1$, E_1 is repellent. When $0<v_2<2\beta_2/\alpha_2$, $E_2=(0,\alpha_2/2)$ is a saddle point; when $v_2>2\beta_2/\alpha_2$, E_2 is repellent. When (v_1,v_2) is in the stability region S, the Nash equilibrium E_* is locally asymptotically stable.*

Proposition 2. *When (v_1,v_2) is in the stability region S, for the fixed $0<v_1<v^-$, when v_2 increases, the trajectory of the mapping T_{c-b} is gradually adjusted to reach the Cournot–Bertrand Nash equilibrium E_*, which is the only attractor. Then through Flip bifurcation, E_* loses the stability. When $v^-<v_1<b_1/q_1{}^*$, the trajectory of the mapping T_{c-b} is gradually adjusted to reach the Cournot–Bertrand Nash equilibrium E_*, which is the only attractor. Then through Neimark–Sacker bifurcation, E_* loses the stability. When $b_1/q_1{}^*<v_1<v^+$, the trajectory of the mapping T_{c-b} experiences Flip bifurcation to Cournot–Bertrand Nash equilibrium. Then as v_2 increases, through Neimark–Sacker bifurcation, E_* loses the stability.*

When (v_1,v_2) is not in the stability region S, numerical simulation is used to illustrate the dynamic trajectory of the mapping T_{c-b}.

The economic implication of the above propositions is that when the adjustment speed of each enterprise is not too high, the static Nash equilibrium can be gradually realized through the gradient adjustment mechanism. Even if the participants do not have complete information about the market and are not completely rational, Nash equilibrium can be

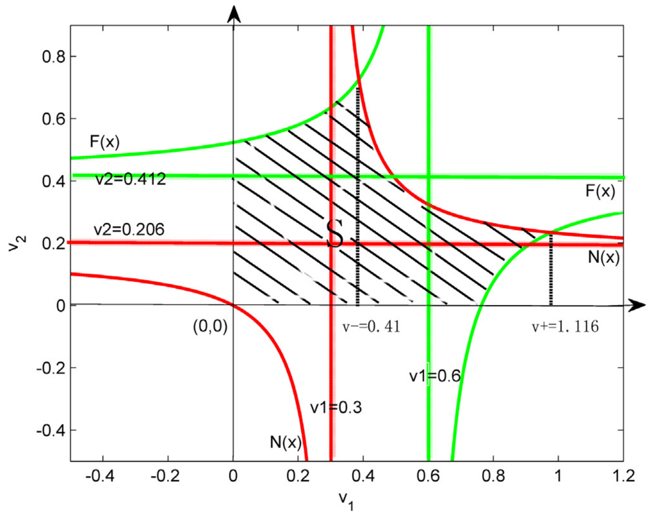

Fig. 2. Local asymptotical stability region S of E_* in Cournot–Bertrand model.

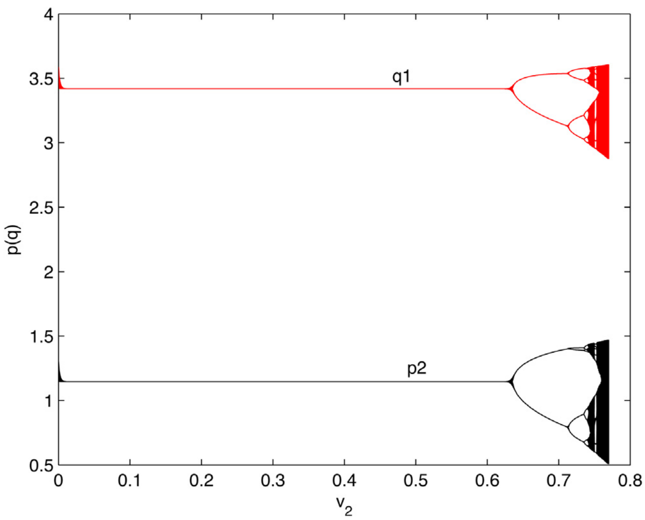

Fig. 3. Flip bifurcation of v_2 in Cournot–Bertrand model ($v_1 = 0.3$).

used to predict the outcome of the game. When the adjustment speed of the participants is larger, the Nash equilibrium will lose its stability. At this time, the Nash equilibrium cannot be used to predict the outcome of the game.

4. The numerical simulation of the local stability of equilibrium in the dynamic Cournot–Bertrand model

In this section, the local stability of equilibrium in a dynamic Cournot–Bertrand model is investigated by numerical simulation. The parameters are given as follows: $\beta_1 = 0.8$, $\beta_2 = 0.6$, $\alpha_1 = 5$, $\alpha_2 = 4$, $r = 0.5$. Thus $a_1 = 4.3478$, $a_2 = 3.0435$, $b_1 = 2.6087$, $b_2 = 3.4782$, $c = 2.1739$, ${q_1}^* = 3.4188$, ${p_2}^* = 1.1453$.

As Fig. 2 shows, the dash area is the local asymptotical stability region S of E_* in Cournot–Bertrand model. When $0 < v_1 < 0.41$, the system experiences equilibrium E_* to Flip bifurcation. When $0.41 < v_1 < 0.763$, the system experiences equilibrium E_* to Neimark–Sacker bifurcation. When $0.763 < v_1 < 1.116$, the system experiences Flip bifurcation, equilibrium E_* to Neimark–Sacker bifurcation. Therefore there are three chaos phenomena from Figs. 3 to 11.

When v_1 is fixed ($v_1 = 0.3$), the Flip bifurcation of v_2 is shown in Fig. 3. When the largest Lyapunov exponent of v_2 is positive in Fig. 4 ($v_2 > 0.74$), there is a chaos in Fig. 3. The strange attractors for $v_1 = 0.3$, $v_2 = 0.76$ is drawn in Fig. 5.

When v_1 is fixed ($v_1 = 0.55$), the Neimark–Sacker bifurcation of v_2 is shown in Fig. 6. When the largest Lyapunov exponent of v_2 is positive in Fig. 7 ($v_2 > 0.44$), there is a chaos in Fig. 6. The strange attractors for $v_1 = 0.55$, $v_2 = 0.45$ is drawn in Fig. 8.

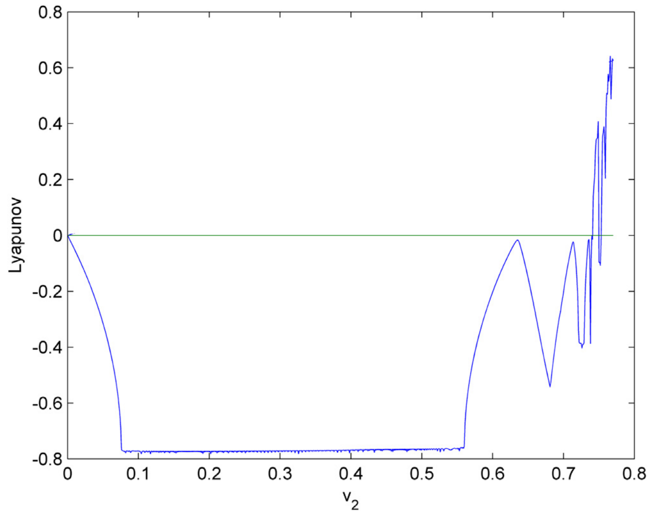

Fig. 4. Lyapunov exponent of v_2 in Cournot–Bertrand model.

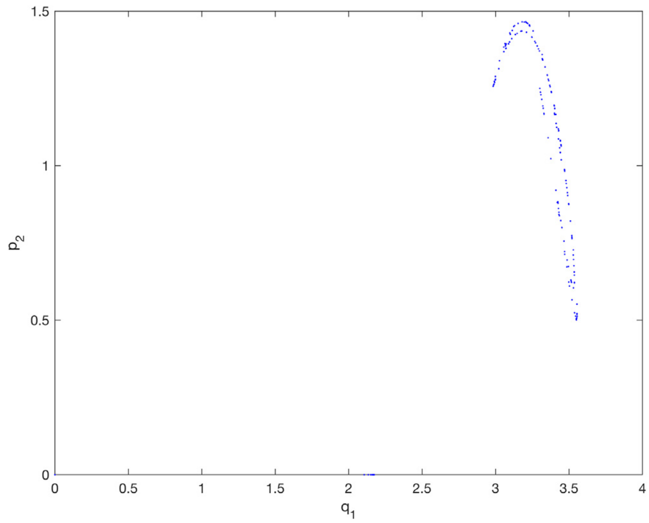

Fig. 5. Strange attractors for $v_1 = 0.3$, $v_2 = 0.76$ in Cournot–Bertrand model.

When v_1 is fixed ($v_1 = 0.95$), the Flip to Neimark–Sacker bifurcation of v_2 is shown in Fig. 9. When the largest Lyapunov exponent of v_2 is positive in Fig. 10 ($0 < v_2 < 0.01$, $v_2 > 0.31$), there is a chaos in Fig. 9. The strange attractors for $v_1 = 0.95$, $v_2 = 0.34$ is drawn in Fig. 11.

The trajectories of three strange attractors are very different, which present rich and colorful dynamics phenomena.

5. The global stability of equilibrium of the dynamic Cournot–Bertrand model

In the previous research on the system stability of the dynamic duopoly games, most scholars have analyzed the local stability of the attractors. However, in recent references, the global stability of the attractors attracts more concern. In this paper, the mapping T_{c-b} which is given by the evolution Eq. (7) of the dynamic Cournot–Bertrand model is an irreversible mapping, that is for the fixed q_1 and p_2, their images $q_1{}'$ and $p_2{}'$ are determined uniquely by formula (7). However, for a point $(q_1{}', p_2{}')$ in the phase space, their preimages (q_1, p_2) cannot be determined uniquely. For the global stability of attractors of the irreversible mapping, invariant set, critical curves and basin of attraction are needed.

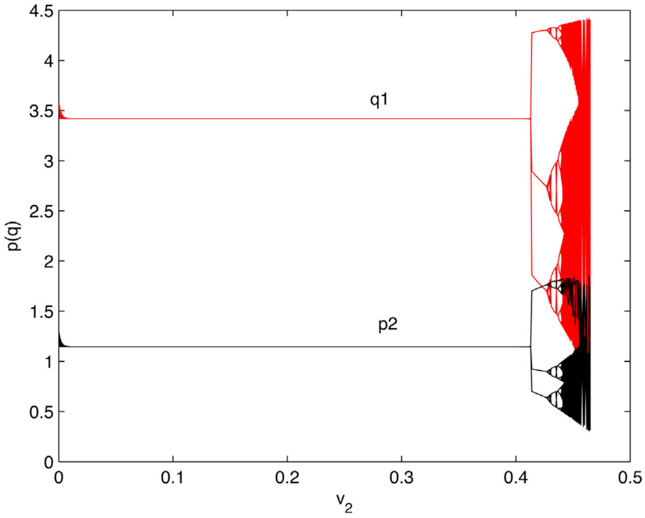

Fig. 6. Neimark–Sacker bifurcation of v_2 in Cournot–Bertrand model ($v_1 = 0.55$).

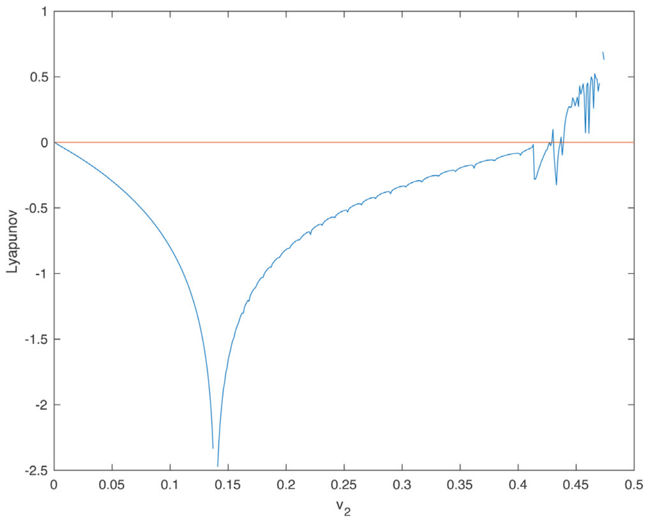

Fig. 7. Lyapunov exponent of v_2 in Cournot–Bertrand model.

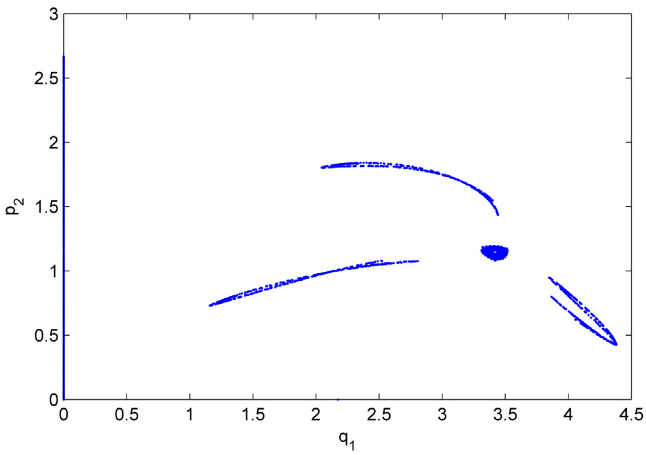

Fig. 8. Strange attractors for $v_1 = 0.55$, $v_2 = 0.45$ in Cournot–Bertrand model.

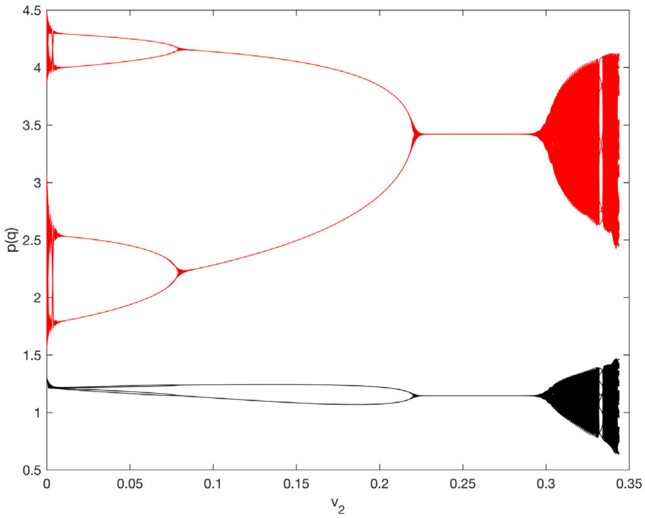

Fig. 9. Flip to Neimark–Sacker bifurcation of v_2 in Cournot–Bertrand model ($v_1 = 0.95$).

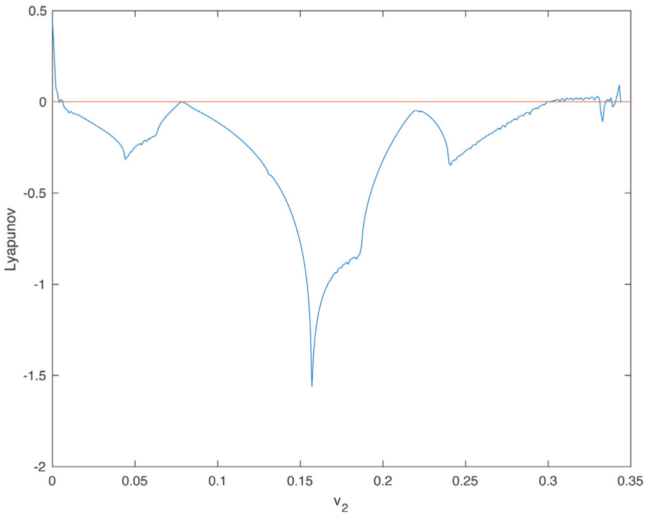

Fig. 10. Lyapunov exponent of v_2 in Cournot–Bertrand model.

5.1. The dynamics of invariant axes in the dynamic Cournot–Bertrand model

Easy to know, for the mapping T_{c-b}, the vertical axis $q_1 = 0$ and horizontal axis $p_2 = 0$ are invariant sets. $f_1(q_1)$ is represented by the mapping T_{c-b} restricted to the horizontal axis $p_2 = 0$. $f_2(p_2)$ is represented by the mapping T_{c-b} restricted to the vertical axis $q_1 = 0$.

$f_1(q_1) = q_1 + v_1 q_1(a_1 - 2q_1)/b_1 = (1 + V_1 a_1)q_1(1 - 2V_1 q_1/(1 + V_1 a_1))$, where $V_1 = v_1/b_1$.

Let $Z = 2V_1 q_1/(1 + V_1 a_1)$ or $q_1 = (1 + V_1 a_1)Z/2V_1$. Thus $f_1(q_1)$ is conjugated to the standard Logistic mapping $Z' = \mu z(1 - z)$, where $\mu = 1 + a_1 V_1$.

We have dual conclusions as follows:

$f_2(p_2) = p_2 + v_2 p_2(\alpha_2 - 2p_2)/\beta_2 = (1 + V_2\alpha_2)p_2(1 - 2V_2 p_2/(1 + V_2\alpha_2))$, where $V_2 = v_2/\beta_2$.

Let $Z = 2V_2 p_2/(1 + V_2\alpha_2)$ or $p_2 = (1 + V_2\alpha_2)Z/2V_2$. Thus $f_2(p_2)$ is conjugated to the standard Logistic mapping $Z' = \mu z(1 - z)$, where $\mu = 1 + \alpha_2 V_2$.

From the standard Logistic mapping, the properties of $f_1(q_1)$ are concluded:

(a) When $0 < V_1 a_1 < 2 (\Leftrightarrow 1 < \mu < 3)$, the equilibrium $E_1 = (a_1/2, 0)$ is the only attractor of asymptotic stability, whose basin of attraction is $\mathsf{B}(E_1) = (E_0, A_1)$, where $A_1 = ((1 + a_1 V_1)/2V_1, 0)$ ($Z = 1$ in conjugate transformation). Considering the feasibility of (q_1, p_2), the basin of attraction which has the economic meaning is $\mathsf{B}(E_1) = (E_0, A_1) \cap \Omega$.

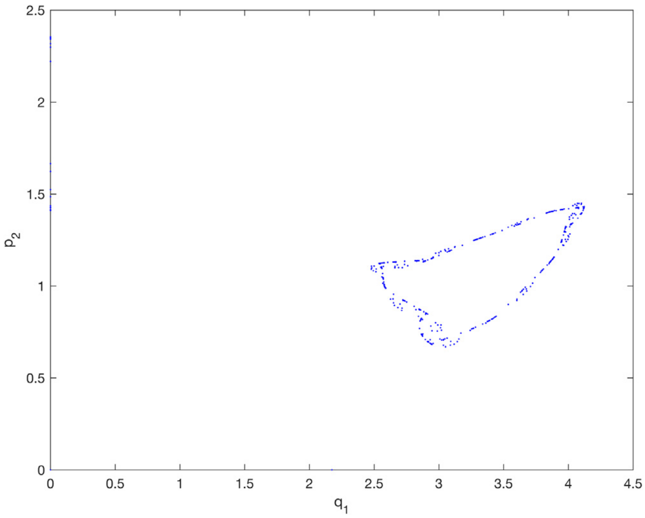

Fig. 11. Strange attractors for $v_1 = 0.95$, $v_2 = 0.34$ in Cournot–Bertrand model.

(b) At $V_1a_1 = 2$, the equilibrium E_1 loses stability through Flip bifurcation, which is defined as $(V_1a_1)_0 = 2$.
(c) When $2 < V_1a_1 < \sqrt{6}$, $f_1(q_1)$ has the only new attractor with a cycle of period 2 whose basin of attraction is still $(E_0, A_1) \cap \Omega$, which is defined as $(V_1a_1)_1 = \sqrt{6}$.
(d) At $V_1a_1 = \sqrt{6}$, the attractor of (c) loses stability through the bifurcation. Thus there is a sequence of bifurcations $(V_1a_1)_n$, $n = 0, 1, 2, \ldots$, when $(V_1a_1)_{n-1} < V_1a_1 < (V_1a_1)_n$, $f_1(q_1)$ has the only stable attractor with a cycle of period 2^n, whose basin of attraction is $(E_0, A_1) \cap \Omega$. Simultaneously, $\lim_{n\to\infty}(V_1a_1)_n = (V_1a_1)_\infty \approx 2.5699456\cdots$
(e) When $(V_1a_1)_\infty < V_1a_1 < 3$, $f_1(q_1)$ has a chaotic attractor in $[(\frac{(1+V_1a_1)^3(3-V_1a_1)}{32V_1}, 0), (\frac{(1+V_1a_1)^2}{8V_1}, 0)] \cap \Omega$.
(f) When $V_1a_1 > 3$, the trajectory of $f_1(q_1)$ starting from $[E_0, A_1] \cap \Omega$ diverges.

Similarly, the dynamic properties of $f_2(p_2)$ are available.

(a)′ When $0 < V_2\alpha_2 < 2(\Leftrightarrow 1 < \mu < 3)$, the equilibrium $E_2 = (0, \alpha_2/2)$ is the only attractor of asymptotic stability, whose basin of attraction is $\mathrm{B}(E_2) = (E_0, A_2) \cap \Omega$, where $A_2 = (0, (1 + \alpha_2V_2)/2V_2)$.
(b)′ At $V_2\alpha_2 = 2$, the equilibrium E_2 loses stability through Flip bifurcation, which is defined as $(V_2\alpha_2)_0 = 2$.
(c)′ When $2 < V_2\alpha_2 < \sqrt{6}$, $f_2(p_2)$ has the only new attractor with a cycle of period 2 whose basin of attraction is still $(E_0, A_2) \cap \Omega$, which is defined as $(V_2\alpha_2)_1 = \sqrt{6}$.
(d)′ At $V_2\alpha_2 = \sqrt{6}$, the attractor of (c)' loses stability through the bifurcation. A sequence of bifurcations $(V_2\alpha_2)_n$, $n = 0, 1, 2, \ldots$, when $(V_2\alpha_2)_{n-1} < V_2\alpha_2 < (V_2\alpha_2)_n$, $f_2(p_2)$ has the only stable attractor with a cycle of period 2^n, whose basin of attraction is $(E_0, A_2) \cap \Omega$. Simultaneously, $\lim_{n\to\infty}(V_2\alpha_2)_n = (V_2\alpha_2)_\infty \approx 2.5699456\cdots$
(e)′ When $(V_2\alpha_2)_\infty < V_2\alpha_2 < 3$, $f_2(p_2)$ has a chaotic attractor in $[0, (\frac{(1+V_2\alpha_2)^3(3-V_2\alpha_2)}{32V_2}), (0, \frac{(1+V_2\alpha_2)^2}{8V_2})] \cap \Omega$.
(f)′ When $V_2\alpha_2 > 3$, the trajectory of $f_2(p_2)$ starting from $[E_0, A_2] \cap \Omega$ diverges.

5.2. The critical curves

The critical curve of two-dimensional map is the extension of the critical value (extremum) of one-dimensional map. It is an important tool to analyze the global stability of the attractor in two-dimensional irreversible mapping. Although the preimages of all points in the phase plane of the two-dimensional non-invertible mapping cannot be calculate, we can divide the phase plane into different regions by the critical curves, which makes the point (q_1, p_2) in the same region has the same number of preimages. The critical curve LC is the boundary curve between two regions. To obtain the critical curve LC of two-dimensional map, the preimage of rank-1 LC_{-1} should be first determined, which is the extension of critical point (extremum) in one-dimensional map. For a differentiable two-dimensional map, the determinant of Jacobian matrix is 0, that is $LC_{-1} \subseteq \{(q_1, p_2) \in R^2 \,|DetJ(q_1, p_2) = 0\}$. For the mapping T_{c-b}, LC_{-1} satisfies:

$$\begin{aligned}&(b_1 + v_1a_1)(\beta_2 + v_2\alpha_2) - (4v_1\beta_2 + b_1v_2r + v_1v_2(4\alpha_2 + a_1r))q_1 - (4b_1v_2 - \beta_2v_1c\\&+v_1v_2(4a_1 - \alpha_2c))p_2 + 16v_1v_2q_1p_2 + 4v_1v_2rq_1{}^2 - 4v_1v_2cp_2{}^2 = 0\end{aligned} \tag{9}$$

It is generally a hyperbola with two branches LC^a_{-1} and LC^b_{-1}. Thus the critical curve of T_{c-b} is $LC = T_{c-b}(LC_{-1}) = T_{c-b}(LC^a_{-1}) \cup T_{c-b}(LC^b_{-1}) \triangleq LC^a \cup LC^b$.

The expression of LC could not be available, however the intersection point coordinates of LC and $q_1 = 0$, LC and $p_2 = 0$ could be calculated.

For a point $(0, x)$ on the p_2 axis, $0 < x < \frac{1+v_2\alpha_2}{2v_2}$. Where $\frac{1+v_2\alpha_2}{2v_2}$ is the ordinate of A_2. Simultaneously A_2 is a preimage of E_0. From the mapping T_{c-b} in formula (7), the preimage of $(0, x)$ is solved by the equations:

$$\begin{cases} 0 = q_1(1 + V_1(a_1 + cp_2 - 2q_1)) & \text{(a)} \\ x = (1 + V_2\alpha_2)p_2 - 2V_2{p_2}^2 - rV_2q_1p_2 & \text{(b)} \end{cases} \tag{10}$$

The solution of (10)(a) satisfies $q_1 = 0$ or $1 + V_1(a_1 + cp_2 - 2q_1) = 0$, which is equivalent to

$$q_1 = (1 + V_1(a_1 + cp_2))/2V_1 \tag{11}$$

For convenience, the line represented by formula (11) is denoted as ${w_2}^{-1}$, the line segment $[E_0A_2]$ is denoted as w_2. Similarly, for the point $(x, 0)$ on $p_2 = 0$, $(0 < x < (1 + v_1a_1)/2v_1)$, the preimage of $(x, 0)$ is solved by the equations:

$$\begin{cases} p_2(1 + V_2(\alpha_2 - rq_1 - 2p_2)) = 0 & \text{(a)} \\ (1 + V_1a_1)q_1 - 2V_1{q_1}^2 + cV_1p_2q_1 = x & \text{(b)} \end{cases} \tag{12}$$

The solution of (12)(a) satisfies $p_2 = 0$ or $1 + V_2(\alpha_2 - rq_1 - 2p_2) = 0$, which is equivalent to

$$p_2 = 1 + V_2(\alpha_2 - rq_1)/2V_2 \tag{13}$$

For convenience, the line represented by formula (13) is denoted as ${w_1}^{-1}$, the line segment $[E_0, A_1]$ is denoted as w_1. With respect to the critical curve of the mapping, we can get the following propositions.

Proposition 3. *The two intersections of the critical curve LC of the mapping T_{c-b} and p_2-axis are ${p_2}^{(1)}$, ${p_2}^{(2)}$, respectively. The two intersections of the critical curve LC of the mapping T_{c-b} and q_1-axis are ${q_1}^{(1)}$, ${q_1}^{(2)}$, respectively.*

For the point $(x, 0)$ on q_1-axis $(0 < x < (1 + v_1a_1)/a_1v_1)$, when $x > \max\left\{{q_1}^{(1)}, {q_1}^{(2)}\right\}$, $(x, 0)$ has no preimage. When $\min\left\{{q_1}^{(1)}, {q_1}^{(2)}\right\} < x < \max\left\{{q_1}^{(1)}, {q_1}^{(2)}\right\}$, $(x, 0)$ has two preimages. When $x < \min\left\{{q_1}^{(1)}, {q_1}^{(2)}\right\}$, $(x, 0)$ has four preimages.

Proof. When $q_1 = 0$, from formula (10)(b), the quadratic equation of p_2 is $2V_2{p_2}^2 - (1 + V_2\alpha_2)p_2 + x = 0$. When the discriminant $\Delta = (1 + V_2\alpha_2)^2 - 8V_2x > 0$, the two roots of the equation are ${p_2}^{+} = (1 + V_2\alpha_2 + \sqrt{\Delta})/4V_2$, ${p_2}^{-} = (1 + V_2\alpha_2 - \sqrt{\Delta})/4V_2$, which illustrates the two preimages of $(0, x)$ on $q_1 = 0$ are $(0, (1 + V_2\alpha_2 + \sqrt{\Delta})/4V_2)$, $(0, (1 + V_2\alpha_2 - \sqrt{\Delta})/4V_2)$.

When $\Delta = 0$, there is only one solution $p_2 = (1 + V_2\alpha_2)/4V_2$, that is $(0, x)$ has only one preimage $(0, (1 + V_2\alpha_2)/4V_2)$.

When $\Delta < 0$, there is no solution or $(0, x)$ has no preimage. While $\Delta \gtrless 0$ is equivalent to $x \lessgtr (1 + V_2\alpha_2)^2/8V_2 = (\beta_2 + v_2\alpha_2)^2/8v_2\beta_2 \triangleq {p_2}^{(1)}$.

When $q_1 = (1 + V_1(a_1 + cp_2))/2V_1$, from formula (10)(b), the quadratic equation of p_2 is $(4 + cr)V_2{p_2}^2/2 - (2V_1 - rV_2 + V_1V_2(2\alpha_2 - ra_1)p_2)/2V_1 + x = 0$. Its discriminant is $\Delta = 2V_1 - rV_2 + V_1V_2(2\alpha_2 - ra_1)^2/4{V_2}^2 - 2(4 + cr)V_2x \gtrless 0$, which is equivalent to

$$\begin{aligned} &x \lessgtr (2V_1 - rV_2 + V_1V_2(2\alpha_2 - ra_1))^2/8{V_1}^2V_2(4 + cr) \\ &= 2\beta_2v_1 - rb_1v_2 + v_1v_2(2a_1 + c\alpha_2)^2/8\beta_2{v_1}^2v_2(4 + cr) \\ &\triangleq {p_2}^{(2)} \end{aligned}$$

When $p_2 = 0$, from formula (12)(b), the quadratic equation of q_1 is $2V_1{q_1}^2 - (1 + V_1a_1)q_1 + x = 0$.

When the discriminant $\Delta = (1 + V_1\alpha_1)^2 - 8V_1x \gtrless 0$, there are two solutions ${q_1}^{\pm} = (1 + V_1a_1 \pm \sqrt{\Delta})/4V_1$ or one solution $q_1 = (1 + V_1a_1)/4V_1$, or no solution.

While $\Delta \gtrless 0$ is equivalent to $x \lessgtr (1 + V_1a_1)^2/8V_1 = (b_1 + v_1a_1)^2/8v_1b_1 \triangleq {q_1}^{(1)}$.

When $p_2 = (1 + V_2(\alpha_2 - rq_1))/2V_2$, from formula (12)(b), the quadratic equation of q_1 is $(4 + cr)V_1{q_1}^2/2 - (2V_2 + cV_1 + V_1V_2(2a_1 + c\alpha_2)q_1)/2V_2 + x = 0$. Its discriminant is $\Delta = 2V_2 + cV_1 + V_1V_2(2a_1 + c\alpha_2)^2/4{V_2}^2 - 2(4 + cr)V_1x \gtrless 0$, which is equivalent to

$$x \underset{>}{\overset{<}{}} (2V_2 + cV_1 + V_1V_2(2a_1 + c\alpha_2))^2/8{V_2}^2V_1(4 + cr)$$
$$= 2b_1v_2 + c\beta_2v_1 + v_1v_2(2a_1 + c\alpha_2)^2/8b_1{v_2}^2v_1(4 + cr)$$
$$\triangleq {q_1}^{(2)}$$

This completes the proof. □

The main function of Proposition 3 can be to divide the same number of preimage regions on the set of feasible strategies of the game, and provide theoretical tools for the analysis of the global stability of attractors.

5.3. The basin of attraction

For the global stability of the attractor A of the mapping T_{c-b}, it is mainly to determine the attraction structure of A. When the economic meaning of T_{c-b} is not considered, for T_{c-b}, the trajectory starting from the initial point far away from the origin is divergent. In our opinion, T_{c-b} has an attractor of infinite point. Therefore, any boundary attractor of T_{c-b} cannot be global attractor. If T_{c-b} has only one boundary attractor A, thus its basin of attraction B(A) and basin of attraction B(∞) of infinite point are complementary. Their boundary of basin of attractions are the same, that is $\partial \mathsf{B}(\infty) = \partial \mathsf{B}(\mathsf{A})$. To obtain $\partial \mathsf{B}(\infty)$, since $w_1 = [E_0, A_1]$, $w_2 = [E_0, A_2]$, easy to know A_1, A_2 are the preimages of E_0. The other two preimages are itself and the intersection A_3 of ${w_1}^{-1}$ and ${w_2}^{-1}$. From formula (11) and (13), the ordinate of A_3 are

$$q_1 = (cv_1\beta_2 + 2v_2b_1 + v_1v_2(2a_1 + c\alpha_2))/v_1v_2(4 + cr),$$
$$p_2 = (2v_1\beta_2 - rv_2b_1 + v_1v_2(2\alpha_2 - ra_1))/v_1v_2(4 + cr).$$

$E_0A_1A_3A_2$ constitutes a quadrangle, whose sides A_1A_3 and A_2A_3 satisfy formula (11) and (13) respectively. The trajectory starting from the outer point of the quadrangle is divergent, therefore the outer part of the quadrangle is contained in B(∞). Since the transverse attraction of T_{c-b} is limited to $[E_0, A_1]$ and $[E_0, A_2]$, that is, the point inside the quadrangle close to the coordinate axes is rejected by the above attractor (refer to 21). From Proposition 3, $T_{c-b}^{-1}(w_1) = w_1 \cup [A_2, A_3]$, $T_{c-b}^{-1}(w_2) = w_2 \cup [A_1, A_3]$. From Bischi et al. [22]

$$\partial \mathsf{B}(\infty) = (\bigcup_{n=0}^{\infty} T_{c-b}^{-n}(w_1)) \cup (\bigcup_{n=0}^{\infty} T_{c-b}^{-n}(w_2)) \tag{14}$$

When $n = 0$, $T_{c-b}(w_1) = w_1$, $T_{c-b}(w_2) = w_2$ in formula (14). The critical curve of $\max\{{q_1}^{(1)}, {q_1}^{(2)}\}$ and $\max\{{p_2}^{(1)}, {p_2}^{(2)}\}$ is the separatrix of the region Z_2 and Z_0. The critical curve of $\min\{{q_1}^{(1)}, {q_1}^{(2)}\}$ and $\min\{{p_2}^{(1)}, {p_2}^{(2)}\}$ is the separatrix of the region Z_2 and Z_4. Where Z_0, Z_2, Z_4 represent the region's preimage number are 0, 2, 4 in the phase space set, respectively. Therefore when $[A_2, A_3] \cup [A_1, A_3] \subseteq Z_0$, the basin of attraction of the bounded attractor A of T_{c-b} is the internal of the quadrangle $E_0A_1A_3A_2$, that is $\mathsf{B}(\mathsf{A}) = \mathrm{int}(E_0A_1A_3A_2)$.

If $([A_1, A_3] \cup [A_2, A_3]) \cap Z_2 \neq \phi$or $([A_1, A_3] \cup [A_2, A_3]) \cap Z_4 \neq \phi$, B(∞) will be in the quadrangle $E_0A_1A_3A_2$ from formula (14). It will destroy the connectivity of the basin of attraction B(A), which makes the basin of attraction B(A) create some "holes". If these "holes" are in the internal of Z_2 and Z_4, there will be more "holes".

When the economic meaning of the map T_{c-b} is considered, T_{c-b} will be constrained by the yield feasible Ω. Therefore we only consider the dynamics of points in Ω.

When the initial point $(q_1, p_2) \in \Omega$ is in ${w_2}^{-1}$or on the right of ${w_2}^{-1}$, from formula (11), $1 + V_1(a_1 + cp_2 - 2q_1) \leq 0$. From formula (7), ${q_1}' = q_1 + V_1(a_1 + cp_2 - 2q_1) \leq 0$, and ${q_1}' = 0$. If and only if the initial point $(q_1, p_2) \in \Omega \cap {w_2}^{-1}$, since ${q_1}' < 0$, which cause firm 1 to quit the market. Therefore ${q_1}' = 0$. The track from (q_1, p_2) is determined by $f_2(p_2)$.

When the initial point $(q_1, p_2) \in \Omega$ is in ${w_1}^{-1}$or above of ${w_1}^{-1}$, from formula (13), $1 + V_2(\alpha_2 - rq_1 - 2p_2) \leq 0$. From formula (7), ${p_2}' = p_2 + V_2p_2(\alpha_2 - rq_1 - 2p_2) \leq 0$, and ${p_2}' = 0$. If and only if the initial point $(q_1, p_2) \in \Omega \cap {w_1}^{-1}$, since ${p_2}' < 0$, which cause firm 2 to quit the market. Therefore ${p_2}' = 0$. The track from (q_1, p_2) is determined by $f_1(q_1)$.

When the initial point $(q_1, p_2) \in \Omega$ is on the right of ${w_2}^{-1}$ and above of ${w_1}^{-1}$, from formula (13) and (7), ${q_1}' = 0$ and ${p_2}' = 0$. The track from $(q_1, p_2) \in \Omega$ will reach the origin.

Only when $(q_1, p_2) \in \Omega$ is in the quadrangle $E_0A_1A_3A_2$, the mapping from the initial point $({q_1}', {p_2}')$ can take a positive.

When the economic meaning is not considered, the initial point $(q_1, p_2) \in \Omega$ is outside the quadrangle $E_0A_1A_3A_2$, the dynamic trajectories will enter the invariant axes, and their motion trajectories are determined by the dynamics on the invariant axes. We need to redefine B(∞): $\mathsf{B}(\infty) = \{(q_1, p_2) \cap \Omega \,\big|\, {q_1}' = 0, \text{ or } {p_2}' = 0\}$.

The results could be still concluded: when $([A_2, A_3] \cup [A_1, A_3]) \cap \Omega \subseteq Z_0$, if the initial point $(q_1, p_2) \in \mathrm{int}(E_0A_1A_3A_2)$, then $\mathsf{B}(\mathsf{A}) = \mathrm{int}(E_0A_1A_3A_2) \cap \Omega$; when $([A_1, A_3] \cup [A_2, A_3]) \cap Z_2 \cap \Omega \neq \phi$ or $([A_1, A_3] \cup [A_2, A_3]) \cap Z_4 \cap \Omega \neq \phi$, B(∞) will enter the interior of the quadrangle $E_0A_1A_3A_2$, which will destroy the connectivity of the attraction domain B(A) and cause the attraction domain B(A) to produce some "holes".

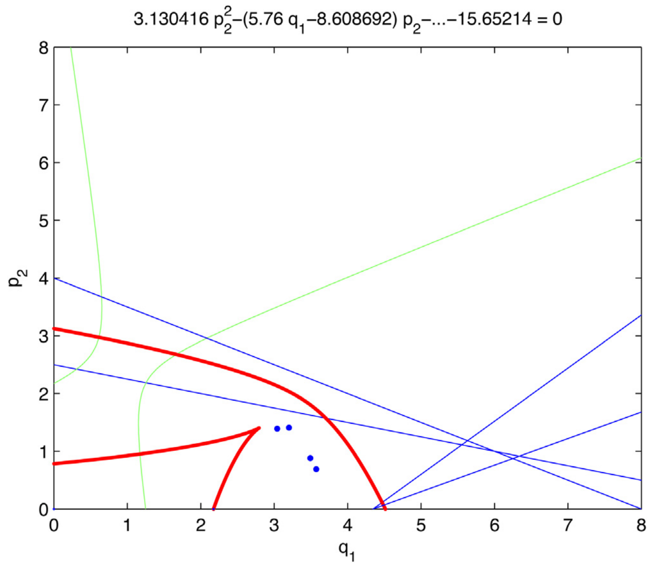

Fig. 12. Critical curves and basin of attraction in Cournot–Bertrand model ($v_1 = v_2 = 0.6$). The rectangle $E_0A_1A_3A_2$ represents equilibria. The feasible set of meaningful area Ω is constrained by the four black lines.

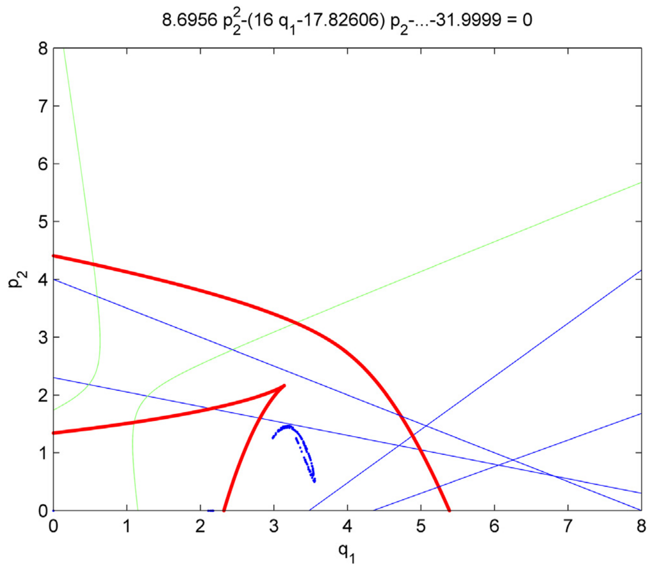

Fig. 13. Critical curves and basin of attraction in Cournot–Bertrand model ($v_1 = v_2 = 1$). The rectangle $E_0A_1A_3A_2$ represents equilibria. The feasible set of meaningful area Ω is constrained by the four black lines.

6. The numerical simulation of the global stability of equilibrium in the dynamic Cournot–Bertrand model

The parameters remain the same: $\beta_1 = 0.8$, $\beta_2 = 0.6$, $\alpha_1 = 5$, $\alpha_2 = 4$, $r = 0.5$. Thus $a_1 = 4.3478$, $a_2 = 3.0435$, $b_1 = 2.6087$, $b_2 = 3.4782$, $c = 2.1739$, $q_1{}^* = 3.4188$, $p_2{}^* = 1.1453$. The intersection of the feasible set Ω and q_1 axis is (4.3478,0); the intersection of the feasible set Ω and p_2 axis is (0,4).

When $v_1 = v_2 = 0.6$, $A_1 = (4.3478, 0)$, $A_2 = (0, 2.5)$, $A_3 = (5.5555, 1.1111)$. The 2^2 period attractors are drawn in Figs. 12, 14 and 16. When $v_1 = v_2 = 1$, $A_1 = (3.47825, 0)$, $A_2 = (0, 2.3)$, $A_3 = (4.7008, 1.1248)$. The strange attractors are drawn in Figs. 13, 15 and 17, which are the same as Figs. 5, 8 and 11, respectively. The phase plane is divided into Z_0, Z_2 and Z_4. The connection of basin of attraction is broken and some "holes" are produced.

The simulations correspond to the results in Section 5.

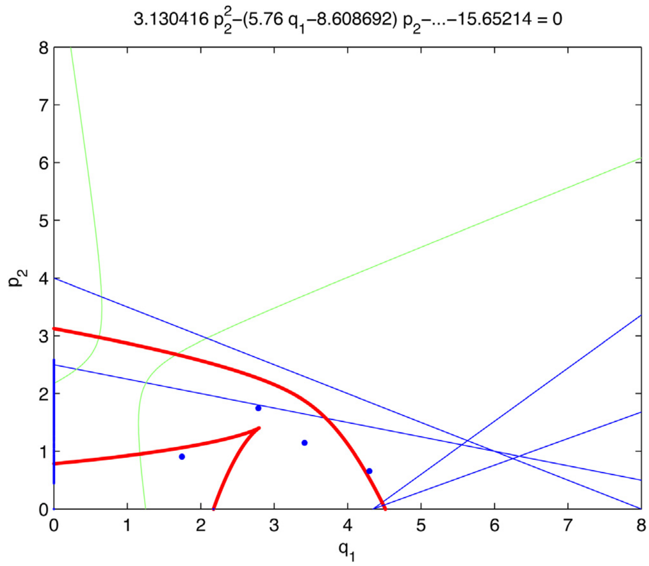

Fig. 14. Critical curves and basin of attraction in Cournot–Bertrand model ($v_1 = v_2 = 0.6$). The rectangle $E_0A_1A_3A_2$ represents equilibria. The feasible set of meaningful area Ω is constrained by the four black lines.

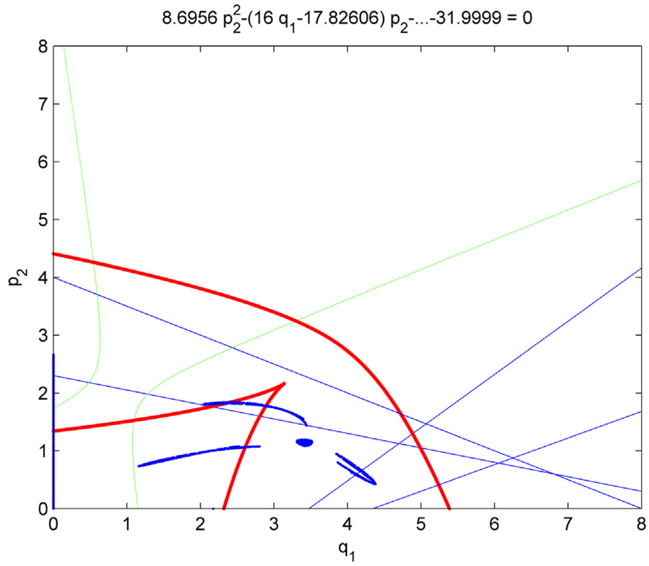

Fig. 15. Critical curves and basin of attraction in Cournot–Bertrand model ($v_1 = v_2 = 1$). The rectangle $E_0A_1A_3A_2$ represents equilibria. The feasible set of meaningful area Ω is constrained by the four black lines.

7. Conclusion

In a Cournot–Bertrand model with products of vertical differentiation, the demand function is deduced from a quadratic utility function. The comparative statics is used to analyze the effect of parameters on equilibrium. A dynamic Cournot–Bertrand game model with bounded rationality is considered. The local stability of the fixed points is investigated by Jury's condition. The theoretical result of the stability region of equilibrium is given. With the increase of the adjustment speed of quantity or price, Flip and Neimark–Sacker bifurcation occur when the adjustment speed passes through the boundary of the stability region. The one-dimensional Logistic mapping is applied in studying the system dynamics property in invariant axes. The critical curve used to give dynamic trajectories on the invariant axes. The critical curve is an important tool to divide the phase plane into several regions Z_0, Z_2 and Z_4. Each region has the same number of preimage, which is beneficial to find the structure of basin of attraction. More complicated chaotic conclusions are obtained by the global stability analysis. Besides the theoretical studies, simulations give more intuitive results. The cycle attractor, chaotic

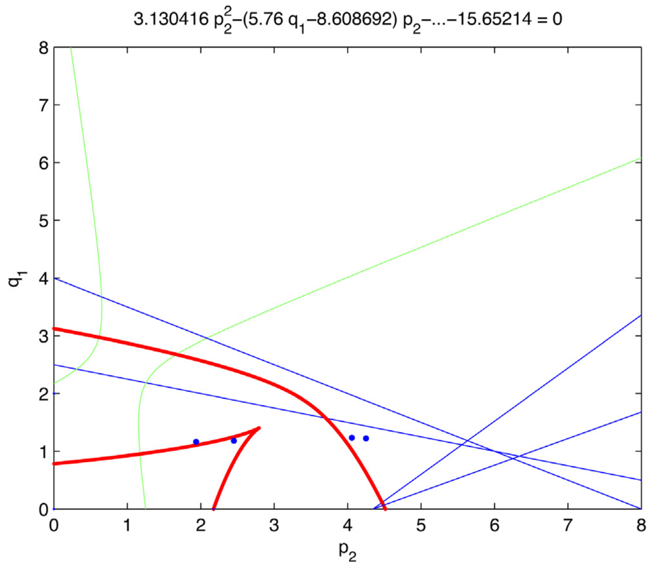

Fig. 16. Critical curves and basin of attraction in Cournot–Bertrand model ($v_1 = v_2 = 0.6$). The rectangle $E_0A_1A_3A_2$ represents equilibria. The feasible set of meaningful area Ω is constrained by the four black lines.

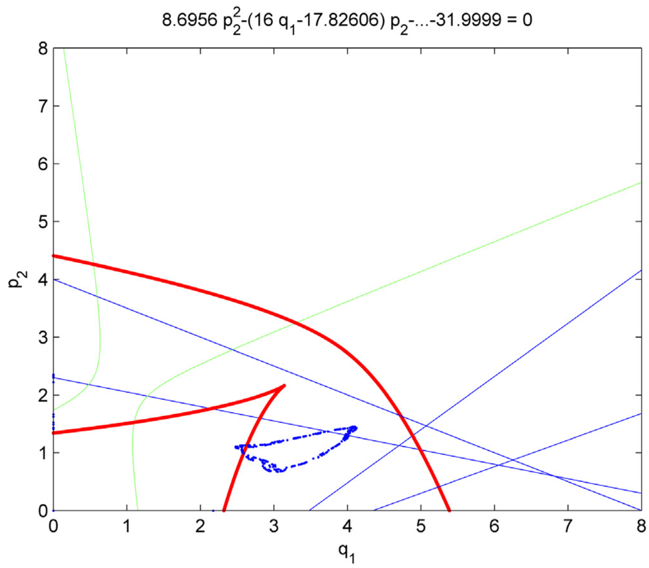

Fig. 17. Critical curves and basin of attraction in Cournot–Bertrand model ($v_1 = v_2 = 1$). The rectangle $E_0A_1A_3A_2$ represents equilibria. The feasible set of meaningful area Ω is constrained by the four black lines.

attractor and the basin of attraction with "holes" are presented. Simulation analysis presents undesirable complicated phenomena.

Funding

This study was funded by Hangzhou Philosophy and Social Science Project (Grant Number Z20JC098).

References

[1] A. Cournot, Recherchessur les Principlesmathematics de la Theoriede la Richesses, Hachette, Paris, 1838.
[2] J. Bertrand, Révue de la TheorieMathematique de la RichesseSociale, J. DesSavants 48 (1883) 499–508.

[3] H.V. Stackelberg, Marktformen Und Gleichgewicht. J, Springer, 1934.
[4] T. Dubiel-Teleszynski, Nonlinear dynamics in a heterogeneous duopoly game with adjusting players and diseconomies of scale, Commun. Nonlinear Sci. Numer. Simul. 16 (2011) 296–308.
[5] Q.G. Yi, X.J. Zeng, Complex dynamics and chaos control of duopoly Bertrand model in Chinese air-conditioning market, Chaos Solitons Fractals 76 (2015) 231–237.
[6] G.I. Bischi, F. Lamantia, D. Radi, An evolutionary Cournot model with limited market knowledge, J. Econ. Behav. Organ. 116 (2015) 219–238.
[7] A.A. Elsadany, Dynamics of a delayed duopoly game with bounded rationality, Math. Comput. Modelling 52 (2010) 1479–1489.
[8] J. Ma, H. Wang, Complex dynamics analysis for a Cournot-Bertrand mixed game model with delayed bounded rationality, Abstr. Appl. Anal. 2013 (2013) 251702, http://dx.doi.org/10.1155/2013/251702.
[9] T. Li, D. Yan, X. Ma, Stability analysis and chaos control of recycling price game model for manufacturers and retailers, Complexity (2019) 2019, http://dx.doi.org/10.1155/2019/3157407.
[10] X. Yang, Y. Peng, Y. Xiao, et al., Nonlinear dynamics of a duopoly Stackelberg game with marginal costs, Chaos Solitons Fractals 123 (2019) 185–191.
[11] Y. Tian, J. Ma, L. Xie, et al., Coordination and control of multi-channel supply chain driven byconsumers' channel preference and sales effort, Chaos Solitons Fractals (2020) 132, http://dx.doi.org/10.1016/j.chaos.2019.109576.
[12] N. Singh, X. Vives, Price and quantity competition in a differentiated duopoly, Rand J. Econ. 15 (4) (1984) 546–554.
[13] C.H. Tremblay, V.J. Tremblay, The Cournot-Bertrand model and the degree of product differentiation, Econ. Lett. 111 (2011) 233–235.
[14] A.K. Naimzada, F. Tramontana, Dynamic properties of a Cournot-Bertrand duopoly game with differentiated product, Econ. Model. 29 (2012) 1436–1439.
[15] A. Semenov, J. Tondji, On the dynamic analysis of Cournot-Bertrand equilibria, Econom. Lett. 183 (2019) 108549.
[16] C.H. Tremblay, V.J. Tremblay, Oligopoly games and the Cournot-Bertrand model: A survey, J. Econ. Surv. 33 (2019) 1–23.
[17] J. Ma, L. Sun, et al., Complexity study on the Cournot-Bertrand mixed duopoly game model with marketshare preference, Chaos 28 (2018) 023101, http://dx.doi.org/10.1063/1.5001353.
[18] H. Wang, J. Ma, Complexity analysis of a Cournot-Bertrand duopoly game model with limited information, Discrete Dyn. Nat. Soc. 2013 (2013) 287371, http://dx.doi.org/10.1155/2013/287371.
[19] H. Wang, J. Ma, Complexity analysis of a Cournot-Bertrand duopoly game with different expectations, Nonlinear Dynam. 78 (2014) 2759–2768.
[20] B. Gao, Y. Du, Equilibrium further studied for combined system of Cournot and Bertrand: A differential approach, Complexity (2020) http://dx.doi.org/10.1155/2020/3160658.
[21] J. Andaluz, G. Jarne, Stability of vertically differentiated Cournot and Bertrand-type models when firms are boundedly rational, Ann. Oper. Res. 238 (1–2) (2016) 1–25.
[22] G.I. Bischi, L. Stefanini, L. Gardini, Synchronization, intermittency and critical curves in duopoly games, Math. Comput. 44 (1998) 559–585.